

FedAli: Personalized Federated Learning with Aligned Prototypes through Optimal Transport

Sannara Ek
 Université Grenoble Alpes
 sannara.ek@gmail.com

Kaile Wang
 Hong Kong Polytechnic University
 21122564r@connect.polyu.hk

François Portet
 Université Grenoble Alpes
 francois.portet@imag.fr

Philippe Lalanda
 Université Grenoble Alpes
 philippe.lalanda@imag.fr

Jiannong Cao
 Hong Kong Polytechnic University
 csjcao@polyu.edu.hk

Abstract

Federated Learning (FL) enables collaborative, personalized model training across multiple devices without sharing raw data, making it ideal for pervasive computing applications that optimize user-centric performances in diverse environments. However, data heterogeneity among clients poses a significant challenge, leading to inconsistencies among trained client models and reduced performance. To address this, we introduce the Alignment with Prototypes (ALP) layers, which align incoming embeddings closer to learnable prototypes through an optimal transport plan. During local training, the ALP layer updates local prototypes and aligns embeddings toward global prototypes aggregated from all clients using our novel FL framework, Federated Alignment (FedAli). For model inferences, embeddings are guided toward local prototypes to better reflect the client’s local data distribution. We evaluate FedAli on heterogeneous sensor-based human activity recognition and vision benchmark datasets, demonstrating that it outperforms existing FL strategies. We publicly release our source code to facilitate reproducibility and furthered research¹.

1 Introduction

Federated Learning (FL) [34] has significantly enhanced the capabilities of edge devices by creating platforms that enable numerous user devices to collaborate in training machine learning models. In this decentralized framework, the training process is distributed across multiple data sources, with only model parameters being communicated instead of raw, privacy-sensitive user data. Despite its promising potential, integrating FL into pervasive computing environments [51], where performance must be user-centric, presents several challenges.

A significant limitation in FL is the heterogeneity inherent in real-world scenarios, where each user’s data distribution may vary significantly due to differences in user behavior, local environments, and other contextual factors [19, 27, 28, 26]. This heterogeneity often leads to client drift, where each user’s model optimization goals diverge, thereby mitigating the benefits of collaboration through FL. Additionally, conventional FL is server-centric, aiming to optimize a single global model to cover a wide range of users, which may need to be more optimal for individual user needs.

While personalized federated learning offers solutions to individual optimum needs, we identify a user-centric requirement for the FL paradigm. Meanwhile, despite the achievement Federated Domain Generalization (FDG) [37, 15] have made, we argue that a personalized client model should also be adaptable to other participated client data distribution. A user-centric FL paradigm necessitates optimization towards the personalization needs of clients in the local environment while enhancing

¹<https://github.com/getalp/FedAli>

their generalization ability to perform reasonably on locally unseen data that differs from local distributions. In order to achieve such goals, we introduce a novel pipeline in the form of a new layer that aligns and regularizes local training embeddings. This process maps input embedding to trainable representative feature vectors, referred to as prototypes, ensuring consistent learning across clients within the federated learning framework. Additionally, we show that this approach significantly increases the robustness of the client’s model against heterogeneous data, promoting better user-centric performance.

Similar to other studies [44, 22, 42, 39], we conduct our experiments in the domain of sensor-based Human Activity Recognition (HAR), where the task is to predict physical activities based on readings from devices with IMU sensors such as smartphones and smartwatches. The domain presents itself as a good test bed for FL applications due to its explicit representation of system heterogeneity (differences in sensing device) and statistical heterogeneity (differences in sensing device placement). Furthermore, the differences among users are idiosyncratic, influenced by their individual peculiarities in performing activities. Particularly in this domain, generalization is essential to provide a broad range of coverage to users who are constantly changing environments and habits in practice. Additionally, we extend our studies to vision datasets, providing a comparison with previous methodologies.

This paper makes the following contributions:

- We identify a crucial yet understudied challenge in user-centric FL under conditions of data heterogeneity, where the model must balance personalization to local datasets while maintaining generalization across other client datasets
- We introduce FedAli, our FL strategy that leverages local prototypes to create global prototypes through a novel Alignment with Prototypes (ALP) layer. This layer enhances alignment and generalization across clients by utilizing an embedding-to-prototype matching mechanism based on optimal transport plan.
- We conduct extensive experiments on two challenging HAR datasets, using clients that are naturally partitioned from individual recorded devices to simulate a realistic and challenging data heterogeneity environment. Furthermore, we extend our evaluation to vision datasets, providing a broader comparison and highlighting the versatility of our approach across different data domains.

2 Preliminaries

The conventional FL framework consists of multiple clients collaboratively training a global model without ever communicating client data [34]. FedAvg algorithm defines the learning objective as:

$$\min_w F(w; \mathcal{D}) = \sum_{k=1}^K \frac{n_k}{n} f_k(w; \mathcal{D}_k) \tag{1}$$

where $F(\cdot)$ is the FL objective, $f_k(\cdot)$ the local loss of client k , w the weights of the global model, K the number of clients, n the total count of data sample and n_k the number of data sample of local client k , \mathcal{D}_k the local dataset of client k and \mathcal{D} the combined datasets of all clients. We note here that \mathcal{D} is actually never available for the global model at the server level in practice (except in simulations to showcase the learning performance of the global model).

As shown in equation 1, conventional FL is server-centric, focusing on achieving good performance for the global (server) model. In this scenario, the server may not handle differences between client models effectively, and unique characteristics or data distributions of individual users may be neglected. To measure such behavior, we argue that we need to explicitly measure the client’s personalization and generalization during FL. That necessitates a shift from the conventional FL optimization

goal, as expressed in equation 1, to equation 2.

$$F(w; \mathcal{D}) = \sum_{c=1}^C \frac{n_c}{n} F_c(w; \mathcal{D}_c), \text{ where } \forall c \min_{w_c} F_c(w_c; \mathcal{D}_c) \text{ such that } H(w_c; \mathcal{D}) \text{ is minimized.} \quad (2)$$

where for each client c , $F_c(\cdot)$ is the local loss and $H(\cdot)$ an error measurement over the entire combined clients dataset \mathcal{D} . The change in expression signifies a user-centric approach, where the main goal is now to have each client c optimize model w_c on local dataset \mathcal{D}_c to increase personalization [18, 55]. Additionally, evaluation function $H(\cdot)$ measures how optimally local model w_c performs on the global dataset \mathcal{D} to estimate generalization performances. Through the collaborative learning trait of FL, client model w_c should also perform well on unseen global datasets \mathcal{D} , which are often dissimilar to local dataset \mathcal{D}_c due to heterogeneity.

While a client’s model is specifically tailored to its local environment, it must also demonstrate robustness to shifts in user local environments, which frequently occur due to changes in user behavior, environmental conditions, or other external factors that cause the data to differ from the original training distribution [40, 20]. These shifts can result in local data resembling another client participating in the FL training, thus expanding the client model’s generalization. However, achieving the right balance between personalization and generalization remains a significant challenge, as models must adapt to local data while still performing well across diverse, unseen environments. This trade-off continues to be a critical research challenge in FL.

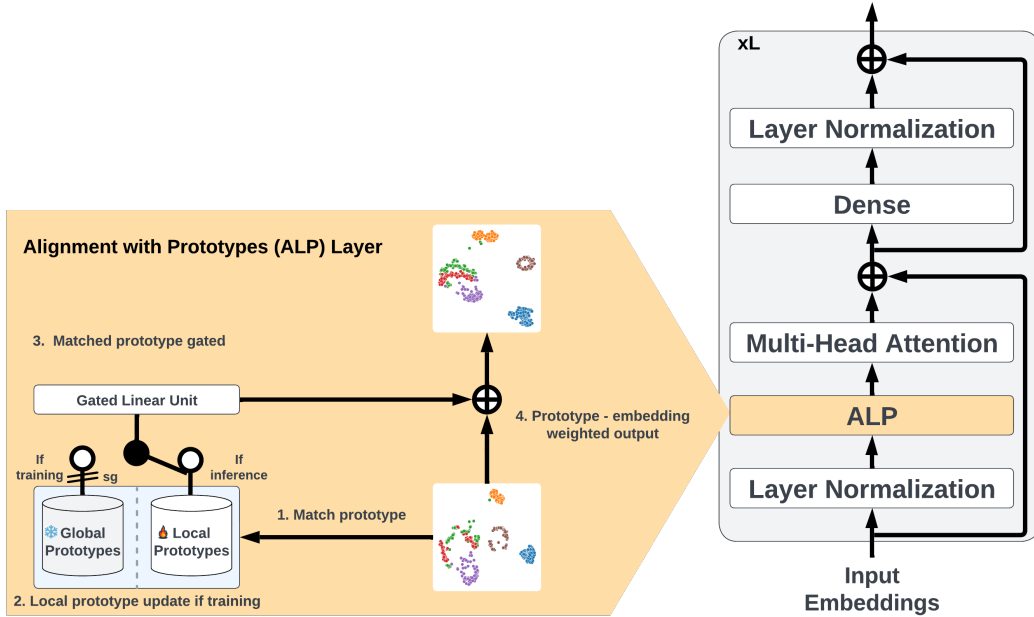


Figure 1: The ALP layer used to align input embeddings illustrated using t-SNE

2.1 Related work

Personalized Federated Learning (PFL) is an extended approach of FL that focuses on customizing the learning process to meet the specific needs, data characteristics, and preferences of individual users [47]. Unlike traditional FL, which aims to create a single global model that fits all users, PFL seeks to tailor models to better align with the unique requirements of each user. Studies in PFL have sought to address the challenges posed by heterogeneity through various regularization techniques. One

prominent method is the use of a mixture of contrastive [5] or distillation techniques [17] as a form of dissimilarity penalization to regularize clients by transferring knowledge from a shared source to local models during training. Various works have proposed different sources for this knowledge transfer, some suggesting direct abstraction of embeddings from intermediate client layers [7, 30, 54, 53], while others employ the global model or models from past clients [1, 25, 23, 29, 6].

More recently, class prototypes have been used to regularize the similarity between different clients [43]. The concept is to obtain a set of prototype vectors, conventionally the barycenters of each class’s embeddings across all clients, that represent the data consistently across the network. Recent work has used these prototypes as a form of global knowledge to help align client’s local training with global objectives [35, 9, 52, 36]. These approaches limit inconsistencies in model training across clients, aiming to ensure that local models contribute positively to improving collaboration despite data heterogeneity. However, these class prototype-based regularization approaches are limited as they require class labels, restricting learning from being solely supervised. Additionally, these methods do not extend to the inference stage, where clients could also benefit from transforming unseen local data into representations consistent with the class prototypes learned during training.

3 Approach

In this work, we introduce the ALignment with Prototypes (ALP) layer, which implements an embeddings-to-prototypes matching process through an optimal transport plan, and our novel FL framework termed Federated Alignment (FedAli) to coordinate the prototypes. Our approach, while functionally similar to other federated learning methods that utilize prototypes to enforce weight similarity during training across clients, offers a distinct advantage. We improve similarity at the embedding level within each transformer encoder block, actively aligning incoming embeddings to be closer to either personalized prototypes during inference or shared generalized prototypes between clients during training.

3.1 Alignment with prototypes (ALP) layer

Here, we detail the process within the ALP layer, as illustrated in figure 1. Consider a batches of sequences of input embeddings $\{x_b\}_{b=1}^B$, where each $x_b \in \mathbb{R}^{Z,d}$ represents a sequence of Z patches/-tokens/frames, each with an embedding dimension of size d . To facilitate prototype alignment and computational efficiency, the batch and sequence dimensions are first collapsed into a single matrix. This transformation reshapes the input from $\mathbb{R}^{B,Z,d}$ to $\mathbb{R}^{B \cdot Z,d}$.

Prototype Matching. The embedding matrix x is subsequently mapped to sets of local and global prototypes. Specifically, we define local prototypes $P_{local} \in \mathbb{R}^{G,d}$ to capture personal embedding semantics and global prototypes $P_{global} \in \mathbb{R}^{G,d}$ to capture shared general embedding semantics between different clients, where G represents the number of prototypes. However, the set of active prototypes P used that will be taken into use does not necessarily consist of both the global and local prototypes and is conditioned on the operational mode of the model:

$$P = \begin{cases} \text{Concat}(P_{local}, P_{global}) & \text{if training} \\ P_{local} & \text{if inference} \end{cases} \quad (3)$$

The computation of the optimal transport plan begins with the construction of an initial cost matrix C_0 , derived from dot product of the L2-normalized input embeddings x_{norm} and L2-normalized active prototypes P_{norm} . This matrix is then iteratively refined into an optimal transport plan using the Sinkhorn-Knopp algorithm [8]:

$$C_0 = \exp\left(\frac{x_{norm} P_{norm}^\top}{\epsilon}\right) \quad (4)$$

$$C_{i+1} = \text{Diag}(u_i) C_i \text{Diag}(v_i)$$

Where $u \in \mathbb{R}^{B \cdot Z}$ and $v \in \mathbb{R}^G$ are scaling vectors used to normalize the rows and columns of similarity matrix C to ensure that the matrix is doubly stochastic. Similar to [4], we found sinkhorn regularization parameter $\epsilon = 0.05$ and 3 iterations to be a good balance of performance and efficiency. Each row in transport plan C quantifies the similarity associated with transporting an input embedding of a patch/token/frame to sets of active prototypes P .

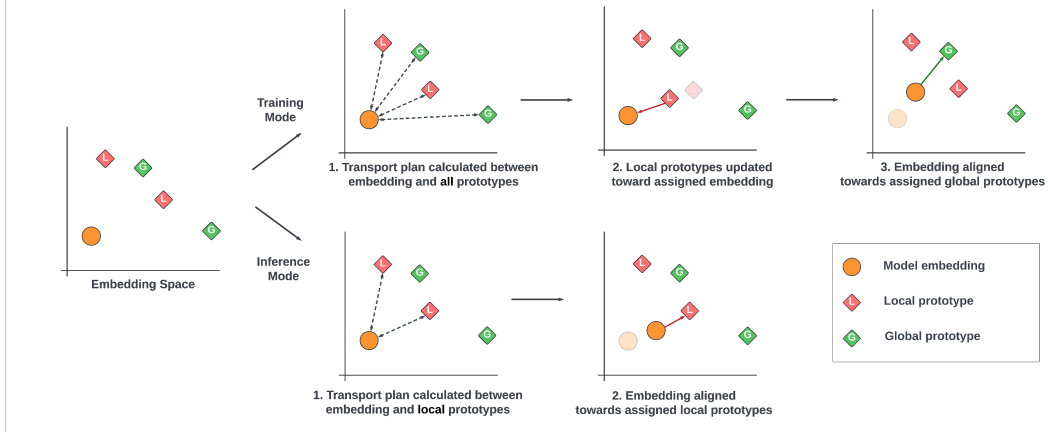


Figure 2: Prototype movements with a single embedding within the ALP layer for each process

During training, the transport plan $C \in \mathbb{R}^{B \cdot Z, 2G}$ encodes the similarity of assigning input embedding to both local prototypes P_{local} and global prototypes P_{global} . To handle these separately, we partition C into C_{local} and C_{global} , each belonging to $\mathbb{R}^{B \cdot Z, G}$. This partitioning is crucial because C_{local} represents the transport cost between input embeddings x and local prototypes, while C_{global} captures the similarity between x and global prototypes. By calculating the transport plan for both prototype sets simultaneously, the approach improves computational efficiency, performing the transport calculation only once. During training, C_{local} is transposed into a prototype-to-embedding plan, which is then used to update the local prototypes, while C_{global} is applied to guide the embeddings toward their assigned global prototypes.

From C_{global} , we perform hard assignments by selecting the maximum similarity for each input embedding, resulting in the global prototype assignments $O_{global} \in \mathbb{N}^{B \cdot Z, G}$. From C_{local}^\top , we obtain a prototype-centric similarity assignment for each local prototype P_{local} to input embeddings x . Local prototypes are soft matched to $\lceil (B \cdot Z) / G \rceil$ input embeddings, to which we obtain local prototype assignments $O_{local}^* \in \mathbb{R}^{G, \lceil (B \cdot Z) / G \rceil}$ which we later use to update local prototypes. The use of multiple soft assignments per prototype proves advantageous when $B \cdot Z > G$, as it allows local prototypes to cover a broader range of input embeddings, especially when the number of prototypes is fewer than the number of embeddings.

When in inference mode, only local prototype transport plan C_{local} is calculated, and local prototype assignments $O_{local} \in \mathbb{N}^{B \cdot F, G}$ is obtained from hard assignments for input embeddings x to local prototypes P_{local} . We note that this design choice, where only P_{local} is used during inference, enhances efficiency in the transport plan calculation. By activating only G prototypes instead of $2G$, the cost of computing the transport plan is reduced.

Prototype updates. Only local prototypes P_{local} , using the local prototype assignments O_{local} , are updated during local training, while global prototypes are updated by through our FL strategy at server level. For each local prototype $p_g \in \mathbb{R}^d$ at index g , we perform a weighted averaging on the normalized similarity value of the assigned $\lceil (B \cdot Z) / G \rceil$ input embeddings to obtain summarized embedding $\hat{x}_g \in \mathbb{R}^d$. Each local prototype p_g at time step t is then updated by:

$$p_g^{t+1} = \gamma p_g^t + (1 - \gamma) \hat{x}_g, \quad (5)$$

where γ represents the decay factor used in the Exponential Moving Average (EMA) for updating the local prototypes. As previously mentioned, global prototypes are not updated locally but are updated at the server level.

Processing selected prototypes. From assignment matrix $O_{global|local}$ based on the current mode (training or inference), we obtain matched prototypes $\hat{P}_{global|local}$ for input embeddings x . These matched prototypes are then processed by a Gated Linear Unit (GLU) [10] to allow the model to regulate the influence of each prototype on the final output. Since the prototypes are not updated by gradients, we apply a stop-gradient function during training, denoted as $sg(\cdot)$, below the GLU layer to ensure that the optimal transport plan calculation will not influence the back-propagation and no gradients are generated for the prototypes. The overall described process here can be formalized as below:

$$P_{GLU} = \begin{cases} GLU(sg(\hat{P}_{global})) & \text{if training} \\ GLU(\hat{P}_{local}) & \text{if inference} \end{cases} \quad (6)$$

Embeddings alignment. Finally, the output of the GLU is applied to the original input projections to align them effectively:

$$\hat{x} = \beta P_{GLU} + (1 - \beta)x \quad (7)$$

Where β is the weighting factor controlling the influence of the prototypes on the input embeddings. After, reshaping back to original output shape $\{\hat{x}_b\}_{b=1}^B$, the aligned embeddings \hat{x} are then L2-normalized similarly to [9].

The movement of the embedding alignment and the local prototype update can be illustratively summarized by figure 2.

4 Federated Alignment (FedAli)

Here, we present Federated Alignment (FedAli) to coordinate clients' prototypes and the aggregation process. As prototypes can be considered as a part of model weights $P \subseteq w$, FedAli aggregation can be implemented in FedAvg's process, as shown in equation 1, with an extension on prototype management. We thus only detail the prototype aggregation pipeline, where after local training, each client sends their updated local weights w_{r+1}^c , that includes updated local prototypes P_{local}^c , to the central server. Note that in practice, the number of prototypes (G) can vary between layers, but for simplicity, assume all ALP layers in encoder blocks $l = 1, 2, \dots, L$ have the same number of prototypes.

As clients in heterogeneous environments tend to update their local prototypes differently to adapt to their data, and we found that coordinate-wise weighted averaging, as used in other studies [48, 52], may combine conflicting local prototypes, leading to less generalized global prototypes. To address this, we employ k-means clustering [31] with the number of clusters set to G , applied to all client's aggregated local prototypes (P_{local}). The converged centroids will be used as the global prototypes P_{global} for the subsequent communication round. Additionally, inspired by a similar approach to enhance stability throughout the communication rounds [38], we use the weighted average of the client's local prototypes $P_{centroid}^{init}$ from FedAvg to initialize the k-means centroids. This process is repeated L times, corresponding to the number of encoder blocks, with each block having a dedicated global prototype.

Algorithm 1 Federated Alignment (FedAli)

```
1: Inputs:  $C$  client,  $R$  communication rounds,  $L$  encoder blocks
2: Initialize  $w_1, P_{global\_1}$ 
3: for each communication round  $r = 1, 2, \dots, R$  do
4:   Server sends  $w_r, P_{global\_r}$  to all clients
5:   for each client  $c \in C$  in parallel do
6:      $w_{r+1}^c, P_{local}^c \leftarrow \text{localTrainALP}(w_r, P_{global\_r})$ 
7:   end for
8:    $w_{r+1}, P_{centroid} \leftarrow \sum_{c=1}^C \frac{n_c}{n} w_{r+1}^c$ 
9:   for each encoder block  $l = 1, 2, \dots, L$  do
10:     $P_{local}^l \leftarrow \{P_{local}^{l,c} \mid c \in [1, C]\}$ 
11:     $P_{global\_r+1}^l \leftarrow \text{KmeanFit}(P_{local}^l, P_{centroid}^l)$ 
12:   end for
13:    $P_{global\_r+1} \leftarrow \{P_{global\_r+1}^l \mid l \in [1, L]\}$ 
14: end for
```

Lastly, before the global model weights are communicated back to the clients, we reset P_{local} to P_{global} to initiate the next round of local training. We empirically observed improved client model consistency by updating the local prototypes P_{local} at the start of each round rather than allowing clients to retain their personalized local prototype. The complete FedAli strategy is detailed in Algorithm 1.

5 Evaluations

5.1 Experimental setups

Datasets. To experiment with different environments with system heterogeneity, we use the **HHAR** dataset [45], which has 9 subjects, each carrying 4 different smartphone models, all mounted on the hip, performing 6 activities. To demonstrate a very statistically heterogeneous environment, we use the **RealWorld** dataset [46] where 8 activities were recorded with 15 diverse subjects, each carrying 7 devices (6 smartphones are of the same model with 1 smartwatch), all in different on-body locations. We do not perform any artificial user partitioning where we consider each unique user and device combination a client for FL in our experiments, such that there are 36 clients and 105 clients when evaluating respectively on the HHAR and RealWorld datasets. Finally, to experiment with an environment with label skew, strong system, and statistical heterogeneity, we combine the clients from the two data sets. We split each client’s local dataset into a 80% / 20% train and test set.

For vision domain, we perform experiments on **CIFAR-10** and **CIFAR-100** [21] which are two image classification datasets with 10 and 100 classes respectively. Each class in CIFAR-10 contains 6000 images. For CIFAR-100, the 100 classes are grouped into 20 superclasses with 500 training images and 100 testing images per class. We applied data partition strategies using Dirichlet distribution as in [33, 24] where we set alpha to 0.3.

Settings We use HART [12] and ViT [11] transformer models, respectively, for the HAR and vision tasks. We train each FL strategy for 600 communication rounds for HAR and 200 communication rounds for vision tasks. Both tasks are trained using the Adam optimizer with a learning rate of 1×10^{-4} , where each client is trained for 5 local epochs with a batch size of 64. Each FL strategy is evaluated using three scores, the Personalization score presents the mean and standard deviation of all client model’s macro F1-score on their respective local test set. The Generalization score evaluates the average client model’s performance on the combined test set from all clients. Since PFL is central to

Table 1: Comparison of FL Strategies on HHAR, RealWorld, and Combined Datasets. Results in **bold** represent the best performance, while results underlined represent the second-best performance.

	HHAR (36 Clients)			RealWorld (105 Clients)			Combined (141 Clients)		
	Personalization	Generalization	Global	Personalization	Generalization	Global	Personalization	Generalization	Global
Centralized	N/A	N/A	97.55	N/A	N/A	89.78	N/A	N/A	91.36
Local	93.84 ± 7.14	33.75 ± 9.21	N/A	91.44 ± 6.06	18.67 ± 3.58	N/A	91.84 ± 6.51	14.20 ± 3.05	N/A
FedAvg	96.88 ± 3.46	75.85 ± 4.97	86.47	90.72 ± 5.85	60.41 ± 3.85	72.47	91.46 ± 6.59	56.24 ± 4.29	68.78
FedPer	95.89 ± 4.68	52.32 ± 9.99	N/A	89.52 ± 7.21	23.10 ± 3.71	N/A	88.12 ± 7.76	17.41 ± 3.36	N/A
FedProx	97.35 ± 2.67	74.97 ± 5.02	86.87	90.97 ± 5.67	<u>60.92 ± 3.69</u>	<u>73.45</u>	91.52 ± 6.65	<u>55.84 ± 4.22</u>	68.56
MOON	97.16 ± 3.63	<u>75.44 ± 5.47</u>	<u>88.03</u>	91.03 ± 5.74	60.26 ± 3.98	74.30	<u>91.86 ± 6.26</u>	55.04 ± 4.85	70.00
FedProto	92.51 ± 9.92	41.66 ± 10.29	N/A	91.55 ± 6.26	21.54 ± 3.69	N/A	91.63 ± 7.59	16.00 ± 3.36	N/A
FedPAC	97.58 ± 2.58	73.05 ± 6.95	N/A	91.06 ± 6.06	34.94 ± 5.99	N/A	91.91 ± 5.97	24.55 ± 5.53	<u>N/A</u>
FedAli	98.15 ± 1.75	81.84 ± 4.81	90.68	90.33 ± 5.77	61.33 ± 3.66	71.50	90.80 ± 6.67	57.25 ± 4.29	<u>68.94</u>

personalization, both scores are obtained using the same client models chosen from the communication round with the highest average Personalization score. Lastly, the Global score evaluates the global model on all clients’ test sets.

The experiments were conducted on a high-performance computing cluster, utilizing Nvidia’s V100 GPUs to parallelize the distributed training process. The HAR experiments were implemented using TensorFlow, while the vision experiments were performed using PyTorch.

Baseline FedAli has been compared against five other FL strategies, including both PFL and regularization approaches, as well as a Local method and a conventional centralized training approach. In the Local method, clients independently train on their local datasets for 200 epochs without any communication with others. In the centralized training approach, we assume that the server has access to all clients’ data and trains the model for 200 epochs, which is sufficient for the model to converge. The FL strategies considered for comparison are FedAvg [34], FedPer [3], FedProx [27] with a tuned proximity term of 0.01, MOON [25] with a contrastive term coefficient tuned to 1.0, FedProto [48] using a prototype regularization term coefficient of 1.0 and FedPAC [52]. For FedAli, after tuning, we set $\beta = 0.2$ and $\gamma = 0.999$, with the number of prototypes decreasing across the 6 encoder blocks, starting from $G = \{2048, 1024, 512, 256, 128, 64\}$, reflecting a progressive reduction in prototypes amount as each layer gets closer to the classification head and the embedding become more coarse-grained.

5.2 Main Results

The performance of the multiple FL strategies on the HHAR, RealWorld, and the combination of the two is reported in table 1. Regarding the compared FL approaches overall, the results consistently show that FedAli excels in generalization with strong personalization and global performance across different datasets, highlighting its robustness in FL environments, especially on the HHAR dataset, where FedAli emerges as the top-performing strategy with a large margin over other approaches, showing the best adaptability across all metrics. MOON performs well across all datasets, particularly excelling in the RealWorld and Combined datasets for global performance. FedAvg and FedProx consistently deliver balanced results, while FedProto and FedPer show limitations in generalization, often leading to overfitting. FedPAC, while competitive in terms of personalization across all the datasets, declined in terms of generalization. The Local strategy, despite strong personalization, consistently underperforms in generalization, highlighting the trade-off between local adaptability and broader applicability. While the centralized results can exhibit the best overall results in our findings here, they are not directly comparable to the FL strategies due to the need to communicate and aggregate user data. It here serves as the upper bound performances that can be reached.

The comparative results in table 2 show that FedAli, within the domain vision as well, outperforms most baseline methods past methods. FedProx exhibits strong generalization, particularly with a larger number of clients across both datasets. FedPAC also shows competitive performance, especially in the personalized evaluation of CIFAR100. In contrast, FedPer and FedProto yield limited results

Table 2: Comparison of FL Strategies on CIFAR10 and CIFAR100 with 20 and 50 clients. Results in **bold** represent the best performance, while results underlined represent the second-best performance.

	CIFAR10 (20 Clients)			CIFAR10 (50 Clients)			CIFAR100 (20 Clients)			CIFAR100 (50 Clients)		
	Per.	Gen.	Global	Per.	Gen.	Global	Per.	Gen.	Global	Per.	Gen.	Global
FedAvg	76.91 ± 6	43.29 ± 7	64.41	78.29 ± 11	34.62 ± 9	59.78	42.88 ± 4	19.11 ± 1	<u>32.55</u>	40.93 ± 5	17.39 ± 1	31.29
FedPer	76.05 ± 6	39.57 ± 6	N/A	75.76 ± 12	29.64 ± 7	N/A	37.19 ± 5	11.39 ± 1	N/A	30.36 ± 4	8.34 ± 1	N/A
FedProx	75.14 ± 5	43.21 ± 6	61.94	<u>78.57 ± 10</u>	35.64 ± 7	<u>57.88</u>	41.66 ± 4	<u>20.47 ± 1</u>	30.90	<u>42.04 ± 4</u>	18.84 ± 1	31.49
MOON	63.08 ± 8	25.14 ± 3	18.44	66.79 ± 15	19.44 ± 5	20.52	29.40 ± 5	7.48 ± 1	4.48	25.08 ± 4	5.45 ± 1	4.22
FedProto	69.16 ± 6	29.60 ± 4	N/A	70.61 ± 14	22.61 ± 5	N/A	30.99 ± 6	9.24 ± 1	N/A	22.21 ± 5	5.99 ± 1	N/A
FedPAC	74.66 ± 6	38.45 ± 6	N/A	76.80 ± 11	30.87 ± 8	N/A	<u>45.33 ± 4</u>	16.50 ± 1	N/A	38.66 ± 4	16.23 ± 1	N/A
FedAli	77.68 ± 5	43.14 ± 6	64.46	79.89 ± 10	<u>34.90 ± 9</u>	57.39	46.49 ± 5	21.24 ± 1	35.45	43.70 ± 4	<u>18.30 ± 1</u>	32.71

in heterogeneous settings, particularly in generalization. While FedAvg performs well on CIFAR10, it struggles on CIFAR100 due to increased data heterogeneity. Overall, FedAli strikes a strong balance between generalization and personalization, highlighting its effectiveness in vision tasks.

Pretraining. We demonstrate that by regularizing embeddings through the ALP layer without relying on a new loss term for alignments, the ALP layer can be applied to any task, including those without labels. We pre-trained HART and local prototypes in a self-supervised learning manner using MAE [16] on five other public datasets [14, 32, 41, 2, 49]. Results presented in figure 3 shows that FedAli, on the HHAR clients, starting the learning from a pre-trained model with prototypes can significantly improve generalization (more than 20% gain) and global performances (more than 11% gain) while retraining personalization performance and reaching a smaller standard deviation.

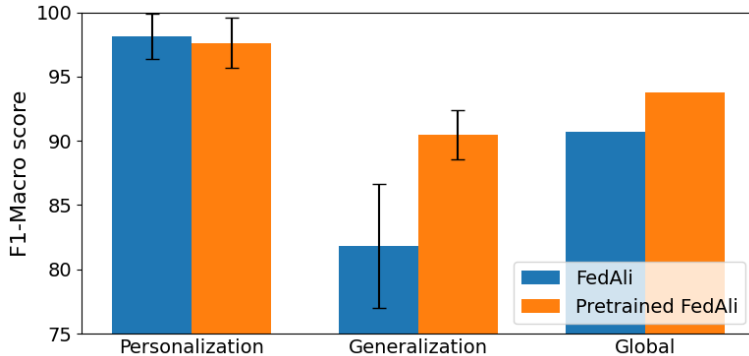


Figure 3: Performance gains using a pretrained model on the HHAR dataset

Communication and computation overhead. Table 3 presents the training time, storage requirement, and communication cost of all the compared FL strategies relative to FedAvg in our configurations. We show that while FedAli indeed has more parameters and higher communication overhead due to the prototypes, they are relatively much faster than other recent FL strategies that rely on contrastive techniques during training. Additionally, unlike other prototype-based methods, FedAli does not require clients to store all class representations from their local datasets to compute local prototypes (Data. Rep), potentially reducing local storage and memory costs, especially at scale on larger clients.

Table 3: Local training time, memory footprint, and communication overhead relative to FedAvg on HHAR clients

Method	Local train time ↓	Memory footprint ↓	Comm overhead ↓
FedAVG	0.57 Minutes	5.8 Megabytes	5.8 Megabytes
FedPer	1.00×	1.00×	0.14×
FedProx	2.51×	1.86×	1.00×
MOON	2.30×	2.72×	1.00×
FedProto	2.28×	Data Rep. + 1.00×	0.01×
FedPAC	2.85×	Data Rep. + 1.00×	1.01×
FedAli	1.09×	2.38×	2.38×

5.3 Ablation

The local and global prototypes can be mutually exclusive in our proposed alignment framework. To evaluate the effectiveness of the ALP layer, we performed an ablation study by removing specific components and assessing the impact on the performance of the HHAR clients. We conducted three random runs over 200 communication rounds for each study to ensure the stability of our findings, as presented in Table 4. The results validate the necessity of each part of our framework and highlight the importance of the GLU and the dual prototypes in achieving balanced performance. In addition, we see that without the global prototype’s regularization, there is an increase in Personalization score but a decrease in the Generalization and Global scores. Additionally, we explored other distance metrics, such as cosine similarity or Euclidean distance, to calculate the distance similarity/cost matrix, where our results show that the iterative Sinkhorn-Knopp technique, which operates within the Wasserstein space, gave the most balanced performances. This result can be well attributed to the distribution-to-distribution matching nature associated with optimal transport methods, as opposed to point-to-point conventional approaches, enabling a more holistic usage and update of the prototypes.

Table 4: Ablation study on the HHAR dataset

Method	Personalization	Generalization	Global
Configurations			
FedAli	97.42 ± 3.30	70.04 ± 5.01	82.80 ± 0.47
w/o GLU	97.55 ± 3.40	67.58 ± 5.31	81.22 ± 0.44
w/o Global Prototype	97.60 ± 3.30	68.58 ± 4.97	81.94 ± 0.73
w/o Local Prototype	97.22 ± 3.86	<u>68.73 ± 5.43</u>	82.99 ± 0.73
Distances			
Wasserstein	97.42 ± 3.30	70.04 ± 5.01	82.80 ± 0.47
Cosine	97.61 ± 3.36	69.08 ± 4.82	81.98 ± 0.52
Euclidean	97.12 ± 3.38	<u>69.12 ± 5.02</u>	<u>82.01 ± 0.44</u>

6 Conclusion

In this study, we identify an understudied challenge in user-centric FL under conditions of data heterogeneity, where the model must balance personalization to local datasets while maintaining generalization across other client datasets. To address such issues, we introduced the Alignment with Prototypes (ALP) layer and the Federated Alignment (FedAli) framework to tackle the challenges of client drift in federated learning. Our approach enhances model consistency and performance across diverse clients by leveraging local and global prototypes to align embedding distributions through an

optimal transport plan. Our extensive experiments in the domain of sensor-based Human Activity Recognition (HAR) and conventional vision task of image classification demonstrated that FedAli significantly improves both personalization and generalization compared to existing state-of-the-art methods. Our approach outperforms traditional federated learning techniques by effectively mitigating the adverse effects of statistical and system heterogeneity, ensuring robust model performance even in highly diverse environments. Additionally, we uniquely apply a client-centric evaluation methodology that measures not only the personalization of local models but also their ability to generalize to unseen data distributions from other clients.

While our proposed framework demonstrates significant improvements in generalization in federated learning, several limitations need to be addressed in future work. Regarding privacy concerns, although FedAli inherently offers privacy benefits by keeping data local, the extended transmission of prototypes, which can act as summaries of user feature distributions, may introduce additional vulnerabilities to privacy attacks [50]. While other complementary work to enhance user privacy is applicable, this aspect necessitates further research to ensure robust privacy protection while maintaining the effectiveness of the transmitted prototypes, particularly in scenarios where sensitive data could be inferred from these summaries. In terms of application to other domains, such as those requiring larger models remains to be thoroughly investigated. This future finding is significant for domains that require a higher number of prototypes, where the computational and memory demands could be significantly higher. To address this, exploring scalable approximation methods for calculating the optimal transport plan could be beneficial [13]. By addressing these limitations, future work can enhance the robustness, privacy, and applicability of the proposed framework, making it more versatile for a wide range of federated learning contexts.

References

- [1] Durmus Alp Emre Acar, Yue Zhao, Ruizhao Zhu, Ramon Matas, Matthew Mattina, Paul Whatmough, and Venkatesh Saligrama. Debiasing model updates for improving personalized federated training. In *International conference on machine learning*, pages 21–31. PMLR, 2021.
- [2] Davide Anguita, Alessandro Ghio, Luca Oneto, Xavier Parra, and Jorge Luis Reyes-Ortiz. A public domain dataset for human activity recognition using smartphones. In *21st European Symposium on Artificial Neural Networks, ESANN 2013, Bruges, Belgium, April 24-26, 2013*, 2013.
- [3] Manoj Ghuhana Arivazhagan, Vinay Aggarwal, Aaditya Kumar Singh, and Sunav Choudhary. Federated learning with personalization layers. *arXiv preprint arXiv:1912.00818*, 2019.
- [4] Mathilde Caron, Ishan Misra, Julien Mairal, Priya Goyal, Piotr Bojanowski, and Armand Joulin. Unsupervised learning of visual features by contrasting cluster assignments. *Advances in neural information processing systems*, 33:9912–9924, 2020.
- [5] Ting Chen, Simon Kornblith, Mohammad Norouzi, and Geoffrey Hinton. A simple framework for contrastive learning of visual representations. In *International conference on machine learning*, pages 1597–1607. PMLR, 2020.
- [6] Zihan Chen, Howard Hao Yang, Tony Quek, and Kai Fong Ernest Chong. Spectral co-distillation for personalized federated learning. In *Thirty-seventh Conference on Neural Information Processing Systems*, 2023. URL <https://openreview.net/forum?id=RqjQL08UFC>.
- [7] Liam Collins, Hamed Hassani, Aryan Mokhtari, and Sanjay Shakkottai. Exploiting shared representations for personalized federated learning. In *International conference on machine learning*, pages 2089–2099. PMLR, 2021.
- [8] Marco Cuturi. Sinkhorn distances: Lightspeed computation of optimal transport. *Advances in neural information processing systems*, 26, 2013.
- [9] Yutong Dai, Zeyuan Chen, Junnan Li, Shelby Heinecke, Lichao Sun, and Ran Xu. Tackling data heterogeneity in federated learning with class prototypes. In *Proceedings of the AAAI Conference on Artificial Intelligence*, volume 37, pages 7314–7322, 2023.
- [10] Yann N Dauphin, Angela Fan, Michael Auli, and David Grangier. Language modeling with gated convolutional networks. In *International conference on machine learning*, pages 933–941. PMLR, 2017.
- [11] Alexey Dosovitskiy, Lucas Beyer, Alexander Kolesnikov, Dirk Weissenborn, Xiaohua Zhai, Thomas Unterthiner, Mostafa Dehghani, Matthias Minderer, Georg Heigold, Sylvain Gelly, Jakob Uszkoreit, and Neil Houlsby. An image is worth 16x16 words: Transformers for image recognition at scale. In *International Conference on Learning Representations*, 2021.
- [12] Sannara Ek, François Portet, and Philippe Lalanda. Transformer-based models to deal with heterogeneous environments in human activity recognition. *Personal and Ubiquitous Computing*, pages 1–14, 2023.
- [13] Jean Feydy, Thibault Séjourné, François-Xavier Vialard, Shun-ichi Amari, Alain Trounev, and Gabriel Peyré. Interpolating between optimal transport and mmd using sinkhorn divergences. In *The 22nd International Conference on Artificial Intelligence and Statistics*, pages 2681–2690. PMLR, 2019.

- [14] Hristijan Gjoreski, Mathias Ciliberto, Lin Wang, Francisco Javier Ordonez Morales, Sami Mekki, Stefan Valentin, and Daniel Roggen. The university of sussex-huawei locomotion and transportation dataset for multimodal analytics with mobile devices. *IEEE Access*, 6:42592–42604, 2018.
- [15] Yaming Guo, Kai Guo, Xiaofeng Cao, Tieru Wu, and Yi Chang. Out-of-distribution generalization of federated learning via implicit invariant relationships. In *International Conference on Machine Learning*, pages 11905–11933. PMLR, 2023.
- [16] Kaiming He, Xinlei Chen, Saining Xie, Yanghao Li, Piotr Dollár, and Ross Girshick. Masked autoencoders are scalable vision learners. In *Proceedings of the IEEE/CVF conference on computer vision and pattern recognition*, pages 16000–16009, 2022.
- [17] Geoffrey Hinton, Oriol Vinyals, and Jeff Dean. Distilling the knowledge in a neural network. *arXiv preprint arXiv:1503.02531*, 2015.
- [18] Yihan Jiang, Jakub Konečný, Keith Rush, and Sreeram Kannan. Improving federated learning personalization via model agnostic meta learning. *arXiv preprint arXiv:1909.12488*, 2019.
- [19] Peter Kairouz, H Brendan McMahan, Brendan Avent, Aurélien Bellet, Mehdi Bennis, Arjun Nitin Bhagoji, Kallista Bonawitz, Zachary Charles, Graham Cormode, Rachel Cummings, et al. Advances and open problems in federated learning. *Foundations and trends® in machine learning*, 14(1–2):1–210, 2021.
- [20] Pang Wei Koh, Shiori Sagawa, Henrik Marklund, Sang Michael Xie, Marvin Zhang, Akshay Balsubramani, Weihua Hu, Michihiro Yasunaga, Richard Lanus Phillips, Irena Gao, et al. Wilds: A benchmark of in-the-wild distribution shifts. In *International conference on machine learning*, pages 5637–5664. PMLR, 2021.
- [21] Alex Krizhevsky and Geoffrey Hinton. Learning multiple layers of features from tiny images. Technical Report 0, University of Toronto, Toronto, Ontario, 2009.
- [22] Chenglin Li, Di Niu, Bei Jiang, Xiao Zuo, and Jianming Yang. Meta-har: Federated representation learning for human activity recognition. In *Proceedings of the web conference 2021*, pages 912–922, 2021.
- [23] Daliang Li and Junpu Wang. Fedmd: Heterogenous federated learning via model distillation. *arXiv preprint arXiv:1910.03581*, 2019.
- [24] Hongxia Li, Zhongyi Cai, Jingya Wang, Jiangnan Tang, Weiping Ding, Chin-Teng Lin, and Ye Shi. Fedtp: Federated learning by transformer personalization. *IEEE transactions on neural networks and learning systems*, 2023.
- [25] Qinbin Li, Bingsheng He, and Dawn Song. Model-contrastive federated learning. In *Proceedings of the IEEE/CVF conference on computer vision and pattern recognition*, pages 10713–10722, 2021.
- [26] Qinbin Li, Zeyi Wen, Zhaomin Wu, Sixu Hu, Naibo Wang, Yuan Li, Xu Liu, and Bingsheng He. A survey on federated learning systems: Vision, hype and reality for data privacy and protection. *IEEE Transactions on Knowledge and Data Engineering*, 35(4):3347–3366, 2021.
- [27] Tian Li, Anit Kumar Sahu, Ameet Talwalkar, and Virginia Smith. Federated learning: Challenges, methods, and future directions. *IEEE signal processing magazine*, 37(3):50–60, 2020.
- [28] Tian Li, Anit Kumar Sahu, Manzil Zaheer, Maziar Sanjabi, Ameet Talwalkar, and Virginia Smith. Federated optimization in heterogeneous networks. *Proceedings of Machine learning and systems*, 2:429–450, 2020.

- [29] Tian Li, Shengyuan Hu, Ahmad Beirami, and Virginia Smith. Ditto: Fair and robust federated learning through personalization. In *International conference on machine learning*, pages 6357–6368. PMLR, 2021.
- [30] Paul Pu Liang, Terrance Liu, Liu Ziyin, Nicholas B Allen, Randy P Auerbach, David Brent, Ruslan Salakhutdinov, and Louis-Philippe Morency. Think locally, act globally: Federated learning with local and global representations. *arXiv preprint arXiv:2001.01523*, 2020.
- [31] Stuart Lloyd. Least squares quantization in pcm. *IEEE transactions on information theory*, 28(2):129–137, 1982.
- [32] Mohammad Malekzadeh, Richard G. Clegg, Andrea Cavallaro, and Hamed Haddadi. Protecting sensory data against sensitive inferences. In *Proceedings of the 1st Workshop on Privacy by Design in Distributed Systems, W-P2DS’18*, pages 2:1–2:6, New York, NY, USA, 2018. ACM. ISBN 978-1-4503-5654-1. doi: 10.1145/3195258.3195260. URL <http://doi.acm.org/10.1145/3195258.3195260>.
- [33] Othmane Marfoq, Giovanni Neglia, Richard Vidal, and Laetitia Kameni. Personalized federated learning through local memorization. In *International Conference on Machine Learning*, pages 15070–15092. PMLR, 2022.
- [34] Brendan McMahan, Eider Moore, Daniel Ramage, Seth Hampson, and Blaise Aguera y Arcas. Communication-efficient learning of deep networks from decentralized data. In *Artificial intelligence and statistics*, pages 1273–1282. PMLR, 2017.
- [35] Umberto Michieli and Mete Ozay. Prototype guided federated learning of visual feature representations. *arXiv preprint arXiv:2105.08982*, 2021.
- [36] Xutong Mu, Yulong Shen, Ke Cheng, Xueli Geng, Jiaxuan Fu, Tao Zhang, and Zhiwei Zhang. Fedproc: Prototypical contrastive federated learning on non-iid data. *Future Generation Computer Systems*, 143:93–104, 2023.
- [37] A. Tuan Nguyen, Philip Torr, and Ser-Nam Lim. FedSR: A simple and effective domain generalization method for federated learning. In Alice H. Oh, Alekh Agarwal, Danielle Belgrave, and Kyunghyun Cho, editors, *Advances in Neural Information Processing Systems*, 2022.
- [38] Chamath Palihawadana, Nirmalie Wiratunga, Anjana Wijekoon, and Harsha Kalutarage. Fedsim: Similarity guided model aggregation for federated learning. *Neurocomputing*, 483:432–445, 2022.
- [39] Riccardo Presotto, Gabriele Civitarese, and Claudio Bettini. Fedclar: Federated clustering for personalized sensor-based human activity recognition. In *2022 IEEE international conference on pervasive computing and communications (PerCom)*, pages 227–236. IEEE, 2022.
- [40] Joaquin Quionero-Candela, Masashi Sugiyama, Anton Schwaighofer, and Neil D. Lawrence. *Dataset Shift in Machine Learning*. The MIT Press, 2009. ISBN 0262170051.
- [41] Attila Reiss and Didier Stricker. Introducing a new benchmarked dataset for activity monitoring. In *2012 16th International Symposium on Wearable Computers*, pages 108–109. IEEE, 2012.
- [42] EK Sannara, François Portet, Philippe Lalanda, and VEGA German. A federated learning aggregation algorithm for pervasive computing: Evaluation and comparison. In *2021 IEEE International Conference on Pervasive Computing and Communications (PerCom)*, pages 1–10. IEEE, 2021.
- [43] Jake Snell, Kevin Swersky, and Richard Zemel. Prototypical networks for few-shot learning. *Advances in neural information processing systems*, 30, 2017.

- [44] Konstantin Sozinov, Vladimir Vlassov, and Sarunas Girdzijauskas. Human activity recognition using federated learning. In *2018 IEEE Intl Conf on Parallel & Distributed Processing with Applications, Ubiquitous Computing & Communications, Big Data & Cloud Computing, Social Computing & Networking, Sustainable Computing & Communications (ISPA/IUCC/BDCloud/SocialCom/SustainCom)*, pages 1103–1111. IEEE, 2018.
- [45] Allan Stisen, Henrik Blunck, Sourav Bhattacharya, Thor Siiger Prentow, Mikkel Baun Kjærgaard, Anind Dey, Tobias Sonne, and Mads Møller Jensen. Smart devices are different: Assessing and mitigating mobile sensing heterogeneities for activity recognition. In *Proceedings of the 13th ACM conference on embedded networked sensor systems*, pages 127–140, 2015.
- [46] T. Sztyler and H. Stuckenschmidt. On-body localization of wearable devices: An investigation of position-aware activity recognition. In *2016 IEEE International Conference on Pervasive Computing and Communications (PerCom)*, pages 1–9, 2016.
- [47] Alysia Ziyang Tan, Han Yu, Lizhen Cui, and Qiang Yang. Towards personalized federated learning. *IEEE Transactions on Neural Networks and Learning Systems*, 2022.
- [48] Yue Tan, Guodong Long, Lu Liu, Tianyi Zhou, Qinghua Lu, Jing Jiang, and Chengqi Zhang. Fedproto: Federated prototype learning across heterogeneous clients. In *Proceedings of the AAAI Conference on Artificial Intelligence*, volume 36, pages 8432–8440, 2022.
- [49] George Vavoulas, Charikleia Chatzaki, Thodoris Malliotakis, Matthew Padiaditis, and Manolis Tsiknakis. The mobiaact dataset: Recognition of activities of daily living using smartphones. In *ICT4AgeingWell*, pages 143–151, 2016.
- [50] Zhibo Wang, Mengkai Song, Zhifei Zhang, Yang Song, Qian Wang, and Hairong Qi. Beyond inferring class representatives: User-level privacy leakage from federated learning. In *IEEE INFOCOM 2019-IEEE conference on computer communications*, pages 2512–2520. IEEE, 2019.
- [51] Mark Weiser. The computer for the 21 st century. *Scientific american*, 265(3):94–105, 1991.
- [52] Jian Xu, Xinyi Tong, and Shao-Lun Huang. Personalized federated learning with feature alignment and classifier collaboration. In *The Eleventh International Conference on Learning Representations*, 2023. URL <https://openreview.net/forum?id=SXZr8aDKia>.
- [53] Zhiqin Yang, Yonggang Zhang, Yu Zheng, Xinmei Tian, Hao Peng, Tongliang Liu, and Bo Han. Fedfed: Feature distillation against data heterogeneity in federated learning. *Advances in Neural Information Processing Systems*, 36, 2024.
- [54] Rui Ye, Zhenyang Ni, Chenxin Xu, Jianyu Wang, Siheng Chen, and Yonina C. Eldar. Fedfm: Anchor-based feature matching for data heterogeneity in federated learning. *IEEE Transactions on Signal Processing*, 71:4224–4239, 2023. doi: 10.1109/TSP.2023.3314277.
- [55] Michael Zhang, Karan Sapra, Sanja Fidler, Serena Yeung, and Jose M. Alvarez. Personalized federated learning with first order model optimization. In *International Conference on Learning Representations*, 2021. URL <https://openreview.net/forum?id=ehJqJQk9cw>.

A Pseudo-code of ALP layer

To provide further implementation details, we present the pseudo-code of the ALP layer below, utilizing TensorFlow functions:

```
# ALP Layer Pseudo-Code

def ALP_Layer(input_embeddings, P_local, P_global, training, beta, gamma):
    # Step 1: Collapse input embeddings along batch dimension
    x = reshape(input_embeddings, (-1, input_embeddings.shape[2]))

    # Step 2: Select active prototypes
    if training:
        P = concatenate(P_local, P_global)
    else:
        P = P_local

    # Step 3: Normalize input embeddings and prototypes
    x_norm = L2_normalize(x, axis=1)
    P_norm = L2_normalize(P, axis=1)

    # Step 4: Construct optimal transport plan C using Sinkhorn-Knopp algorithm
    C = exp(dot(x_norm, P_norm.T) / 0.05)
    for _ in range(3):
        C /= sum(C, axis=1, keepdims=True)
        C /= P_norm.shape[0]
        C /= sum(C, axis=0, keepdims=True)
        C /= x_norm.shape[0]
    C *= x_norm.shape[0]

    # Step 5: Compute embedding-prototype matching and update local prototype if training
    if training:
        C_local = C[:, :P_local.shape[0]]
        C_global = C[:, P_local.shape[0]:]
        O_global = argmax(C_global, axis=1)

        # Soft assignment for local prototypes
        O_local = transpose(C_local)
        top_k_indices = top_k(O_local, ceil(x_norm.shape[0] / P_local.shape[0]), sorted=False)
        O_local = gather(O_local, top_k_indices)

        # Update local prototypes using EMA
        weighted_embeddings = gather(x_norm, top_k_indices) * expand_dims(O_local, -1)
        aggregated_embeddings = reduce_sum(weighted_embeddings, axis=1)
        P_local = gamma * P_local + (1 - gamma) * aggregated_embeddings
    else:
        C_local = C[:, :P_local.shape[0]]
        O_local = argmax(C_local, axis=1)

    # Step 6: Match prototypes and process through GLU
    matched_prototypes = gather(P, O_local if not training else O_global)
    P_GLU = GLU(stop_gradient(matched_prototypes))

    # Step 7: Align embeddings
    output = beta * P_GLU + (1 - beta) * x
    output = reshape(output, input_embeddings.shape)
    output = L2_normalize(output, axis=2)

    return output
```

B Sensor-based Human Activity Recognition Datasets

There have been many public datasets available for the sensor-based HAR domain. Below, we detail all the datasets that were used in this study. However, we note again that these datasets are relatively small and encompass large distributions of users and settings. Each dataset factors its uniqueness in feature biases, specific user diversities, recording duration, environment, and devices.

Since datasets were recorded with different sampling rates, we down-sampled them to 50 Hz after applying an Anti-Alias filter. After down-sampling, we only used raw signals normalized with channel-wise z-normalization. We used a window-frame size of 128 (2.56s) with an overlap of 50% over the 6

channels from the 3 axis of accelerometers and 3 axis of gyroscopes. The result input data shape is of size (128, 6) for each sample.

B.1 Heterogeneity Human Activity Recognition

The Heterogeneity Human Activity Recognition (HHAR) dataset consists of 4.5 hours of recorded activities from 9 participants. Each participant wore 8 Android smartphones (2 LG Nexus 4, 2 Samsung Galaxy S3, 2 Samsung Galaxy S3 mini, and 2 Samsung Galaxy S plus) in a tight pouch carried around on the waist and 4 Android smartwatches (2 LG G and 2 Samsung Galaxy Gear) while performing 6 different activities (Biking, Sitting, Standing, Walking, Upstairs, and Downstairs). All 12 devices recorded the activities using accelerometer and gyroscope measurements at their maximum sampling rates ranging from 50 Hz to 200 Hz. The HHAR dataset represents a heterogeneous learning environment due to the variety of devices used in the data collection.

B.2 RealWorld

The RealWorld dataset consists of 18 hours of recorded accelerometer and gyroscope data collected in 2016 from 15 subjects using 6 Samsung Galaxy S4 smartphone and an LG G Watch R placed at 7 different body positions: head, chest, upper arm, waist, forearm, thigh, and shin. The sampling rate was 50 Hz. The subjects performed various activities outdoors without any restrictions, and the data was labeled into 8 activities: Downstairs, Upstairs, Lying, Sitting, Standing, Walking, Jumping, and Running. This dataset aims to simulate the class imbalance that resembles the ones of realistic datasets. For instance, the "standing" activity represents 14% of the data while the "jumping" activity only accounts for 2%.

C Transformer hyper-parameters

We choose a tiny ViT model as backbone network for all baseline methods for fair comparison for the vision. The tiny ViT we selected consists of 6 blocks with 3 attention heads and a corresponding hidden dimension of 192 for all vision datasets. Additionally, we note that HART follows the same hyper-parameter configuration.

For a fair comparison across all baseline methods in the vision tasks, we selected a tiny ViT model as the backbone network. This tiny ViT consists of 6 blocks, each with 3 attention heads and a hidden dimension of 192, applied uniformly across the two vision datasets. Additionally, we note that the HART model uses the same hyper-parameter configuration for our sensor-based HAR datasets.

D Impact of Client Sampling Ratios on Performance.

We evaluated the FL strategies when not all clients participate in the communication rounds, a common scenario for cross-device FL. Specifically, we used the combined dataset environments with client sampling ratios of $\{0.1, 0.2, 0.5\}$, corresponding to $\{14, 28, 70\}$ clients per communication round. To ensure a fair evaluation between the different FL strategies, we pre-computed the random selection of clients.

As shown in figure 4, our experiment focused on FL strategies with a complete global model at the server. Among these, MOON demonstrates effectiveness and modest gains across different sampling rates, while FedAvg's showed better suitability for environments with higher client participation. Fed-Prox, while showing potential for improvement, was the least effective strategy under the evaluated conditions. FedAli exhibits the most consistent performance improvement across various client sampling rates, having the best overall global scores aside from the 0.5 client participation ratio. Also, we highlight that FedAli achieved the highest score of 70.19 when training with only 20% of the available clients.

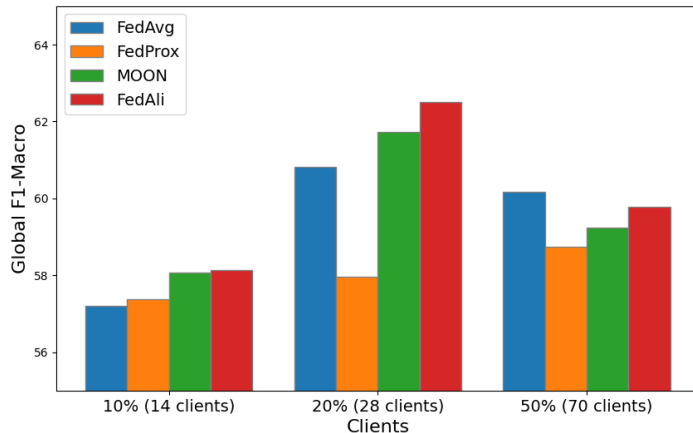


Figure 4: Global performance when sampling from only a subset of clients on the HHAR dataset

E Pretraining with MAE

As mentioned in section 5 of the main content, we pre-train our model using a Masked Autoencoder (MAE). We pre-train the model on 5 publicly available datasets combined (PAMAP2, MotionSense, MobiAct, UCI and the Sussex-Huawei Locomotion Preview). These datasets collectively include a total of 122 subjects, covering 9 distinct device positions and encompassing 18 unique activities. In total, these datasets provide approximately 502 hours of recorded activity data. We pre-train the model, in a centralized manner, for 200 epochs using the Adam optimizer with a learning rate of 3×10^{-4} , a batch size of 128, and a 60% masking ratio to encourage robust feature learning across these diverse datasets and activities.

F Sensitivity analysis

In our experiments, we use a value of $\beta = 0.2$ to control how much the prototype transforms the input embeddings. To demonstrate the influence of this parameter, we tune β for five different values $\{0.1, 0.2, 0.3, 0.4, 0.5\}$ over 3 random runs on the HHAR environment and present our findings in table 5. We see that as β decreases, so does the regularization effect from global prototypes, hence the increase in personalization and decrease in the generalization and global metrics. This property is vice-versa, where we saw a large β institute more significant gains in generalization and global performances but a decrease in personalization. Overall, we found a β value of 0.2, a good balance for our requirements.

Table 5: FedAli with varying β coefficients

β	Personalization	Generalization	Global
0.1	97.63 \pm 3.35	69.03 \pm 5.18	82.27 \pm 0.77
0.2	97.42 \pm 3.30	70.04 \pm 5.01	82.80 \pm 0.47
0.3	97.37 \pm 3.25	70.00 \pm 4.61	83.00 \pm 0.43
0.4	97.13 \pm 3.23	69.97 \pm 4.60	82.88 \pm 0.47
0.5	96.99 \pm 3.28	70.30 \pm 4.87	83.00 \pm 0.31

Next, we study the influence of using different amounts of prototypes. Specifically, we used three settings with prototype counts $\{1024, 512, 256, 128, 64, 32\}$, $\{2048, 1024, 512, 256, 128, 64\}$ and

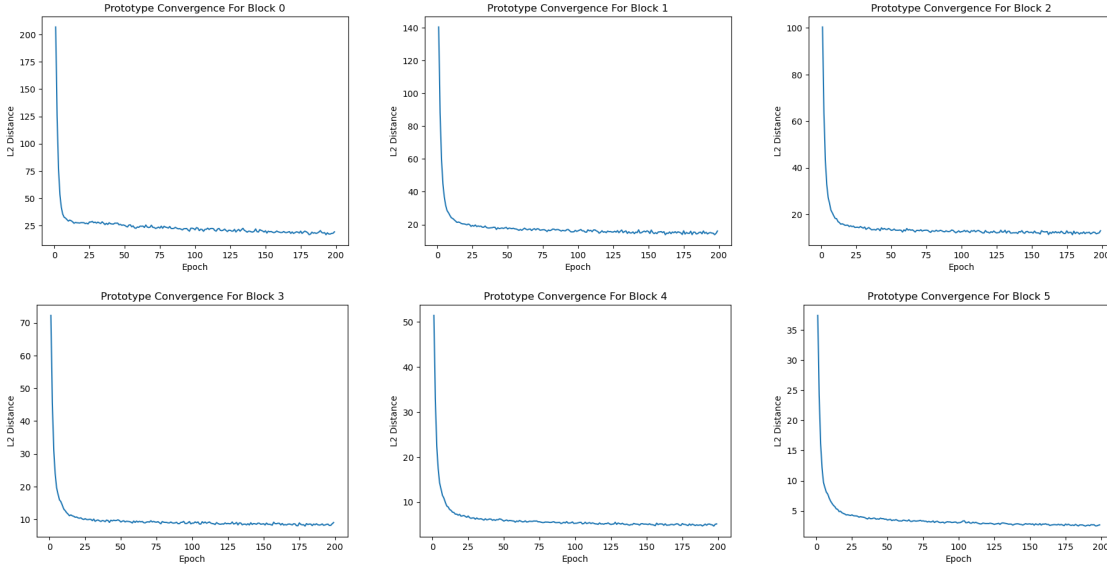


Figure 5: Prototype convergence visualizations for the six encoder blocks. Each subplot represents changes in prototypes for a specific encoder block, demonstrating how prototypes evolve during the convergence process.

{4096, 2048, 1024, 512, 256, 128} where larger counts of prototypes are situated near to the input layer. As presented in table 6, our findings show that in our use case, results are marginally different from one another, whereas the configuration we employed with {2048, 1024, 512, 256, 128, 64} gave a slightly better balance overall.

Table 6: FedAli with different number of prototypes across 6 layers

Prototype Count	Personalization	Generalization	Global
1024, 512, 256, 128, 64, 32	97.48 ± 3.34	<u>69.89 ± 4.81</u>	<u>82.80 ± 0.66</u>
2048, 1024, 512, 256, 128, 64	<u>97.42 ± 3.30</u>	70.04 ± 5.01	82.80 ± 0.47
4096, 2048, 1024, 512, 256, 128	97.38 ± 3.34	69.51 ± 4.82	82.62 ± 0.57

G Prototype convergence

Here, we performed a local experiment to showcase the convergence of the local prototypes trained over 200 epochs instead of the local epoch 5 used in the local training of FedAli. For each prototype p^t , we record the L2 distance to its past counterpart p^{t-1} and report the averaged distance of the learning in Figure 5. Findings show that local prototypes can converge quickly in less than 20 local epochs.